

Results and prospects for $\Upsilon(5S)$ running at B -factories

A. Drutskoy

University of Cincinnati, Cincinnati, OH 45221, USA

Recent results and future prospects for $\Upsilon(5S)$ running at B -factories are discussed. The first Belle measurements with 23.6 fb^{-1} of data taken at the $\Upsilon(5S)$ energy are reported. Eligibility of potential measurements expected with 100 fb^{-1} and 1000 fb^{-1} of data at the $\Upsilon(5S)$ is estimated.

1. INTRODUCTION

During the last several years an opportunity for B_s^0 meson studies at the e^+e^- colliders running at the $\Upsilon(5S)$ resonance has been extensively explored. The first evidence for B_s^0 production at the $\Upsilon(5S)$ was found by the CLEO collaboration [1, 2] using a dataset of 0.42 fb^{-1} collected in 2003. This study indicated that practical B_s^0 measurements at the $\Upsilon(5S)$ are possible with a dataset of at least 20 fb^{-1} , which can be easily collected at B factories running with $\sim 10^{34} \text{ cm}^{-2} \text{ sec}^{-1}$ luminosity. To test the feasibility of a B_s^0 physics program the Belle collaboration collected at the $\Upsilon(5S)$ a dataset of 1.86 fb^{-1} in 2005. After the successful analysis of these data [3, 4], Belle collected a bigger sample of 21.7 fb^{-1} in 2006.

2. EVENT CLASSIFICATION AND FULL B_s^0 EVENT NUMBER DETERMINATION AT THE $\Upsilon(5S)$ RESONANCE

Several $b\bar{b}$ resonances have been observed in the e^+e^- hadronic cross-section in the energy region $\sim 10 \text{ GeV}$ [5]. Among these resonances, the $\Upsilon(4S)$ has a mass slightly above the $B\bar{B}$ production threshold and decays to B^+B^- or $B^0\bar{B}^0$ pairs with almost 100% probability. The next $\Upsilon(5S)$ resonance has a mass exceeding the $B_s^0\bar{B}_s^0$ production threshold and can potentially decay to various final states with the B^+ , B^0 or B_s^0 mesons. If the B_s^0 production rate at the $\Upsilon(5S)$ is not small, the $\Upsilon(5S)$ could play a similar role for comprehensive B_s^0 studies that the $\Upsilon(4S)$ has played for B^+ and B^0 studies.

Hadronic events produced at the energy region of the $\Upsilon(5S)$ can be classified into the three categories (Fig. 1): $\Upsilon(5S)$ resonance events, $b\bar{b}$ continuum events, and $u\bar{u}, d\bar{d}, s\bar{s}, c\bar{c}$ continuum events. The $\Upsilon(5S)$ resonance events and the $b\bar{b}$ continuum events (contributions from these two sources are expected to be about the same) always produce the final states with a B or B_s meson pair, and, therefore, cannot be topologically separated. We define the $b\bar{b}$ continuum and $\Upsilon(5S)$ events collectively as the $b\bar{b}$ events. All $b\bar{b}$ events are expected to hadronize in final states with the $B_{(s)}^{(*)}$ meson pair: $B\bar{B}, B\bar{B}^*, B^*\bar{B}, B^*\bar{B}^*, B\bar{B}\pi, B\bar{B}^*\pi, B^*\bar{B}\pi, B^*\bar{B}^*\pi, B\bar{B}\pi\pi, B_s^0\bar{B}_s^0, B_s^0\bar{B}_s^*, B_s^*\bar{B}_s^0$ or $B_s^*\bar{B}_s^*$. Here B denotes a B^0 or a B^+ meson and \bar{B} denotes a \bar{B}^0 or a B^- meson. The excited states decay to their ground states via $B^* \rightarrow B\gamma$ and $B_s^* \rightarrow B_s^0\gamma$. All possible final states can be separated into B_s and B channel events; the B_s channel events include three channels: with zero, one or two B_s^* mesons.

In order to measure any B_s^0 branching fraction, the number of B_s^0 mesons in a collected $\Upsilon(5S)$ data sample has to be precisely determined. To calculate the B_s^0 number in a dataset with known integrated luminosity L_{int} , the two parameters should be measured in advance: the total $b\bar{b}$ production cross section at the e^+e^- center-of-mass energy $\sigma_{b\bar{b}}^{\Upsilon(5S)}$, and the fraction f_s of B_s^0 events among all $b\bar{b}$ events. Then the number of B_s^0 mesons in a dataset can be calculated as: $N_{B_s^0} = 2 \times L_{\text{int}} \times \sigma_{b\bar{b}}^{\Upsilon(5S)} \times f_s$. For some B_s^0 decays with a high background level it is reasonable to select events only from the $B_s^*\bar{B}_s^*$ channel. In this case the fraction $f_{B_s^*\bar{B}_s^*}$ of $B_s^*\bar{B}_s^*$ events over all $B_{(s)}^{(*)}\bar{B}_{(s)}^{(*)}$ events should be also measured.

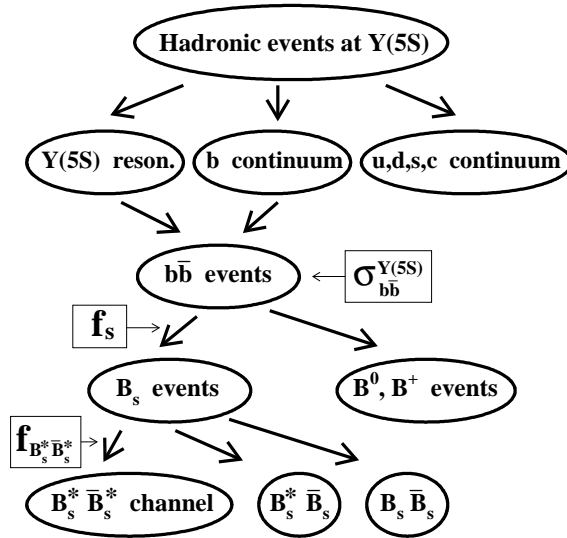


Figure 1: Hadronic event classification at the $\Upsilon(5S)$.

The total $b\bar{b}$ cross section $\sigma_{b\bar{b}}^{\Upsilon(5S)}$ can be determined by comparing the number of hadronic events produced at the $\Upsilon(5S)$ and on the continuum below the $\Upsilon(4S)$ energy. After corrections for the integrated luminosity ratio, the center-of-mass energy ratio and the reconstruction efficiency ratio, the number of events in continuum dataset will reproduce the number of $u\bar{u}$, $d\bar{d}$, $s\bar{s}$ and $c\bar{c}$ continuum events in the $\Upsilon(5S)$ dataset. The dominant systematic uncertainty in the continuum subtraction method comes from the $\Upsilon(5S)$ and continuum luminosity ratio, which is usually calculated using Bhabha events. In the Belle measurement [3] a $\sim 0.4\%$ systematic uncertainty on the integrated luminosity ratio $\mathcal{L}_{5S}/\mathcal{L}_{\text{cont}}$ resulted in the $\sim 5\%$ systematic uncertainty on $\sigma_{b\bar{b}}^{\Upsilon(5S)}$. Probably with higher statistics, the $\Upsilon(5S)$ and continuum dataset integrated luminosity ratio can be better measured comparing D^0 and D_s production at the high momentum region. Unfortunately the $\sigma_{b\bar{b}}^{\Upsilon(5S)}$ uncertainty cannot be essentially reduced below 3% using continuum subtraction methods, and it would become a “core” uncertainty on the full B_s^0 number determination with increasing statistics. By now the $\sigma_{b\bar{b}}^{\Upsilon(5S)}$ value was measured by CLEO [1] to be $(0.301 \pm 0.002 \pm 0.039)$ nb and by Belle [3] to be (0.302 ± 0.015) nb.

The f_s value can be determined by comparing D_s , D^0 or ϕ production in $\Upsilon(5S)$, $\Upsilon(4S)$ and continuum datasets. This method is based on the fact that the D_s and ϕ meson production rate is significantly higher in B_s^0 decays than in $B^{0/+}$ decays (and lower for the D^0 meson). Unfortunately an additional model dependent assumption on the inclusive branching fraction of D_s , ϕ or D^0 production in B_s^0 decays has to be made. Currently the mean PDG value [5], based on CLEO and Belle measurements, is $f_s = (19.5^{+3.0}_{-2.3})\%$. Although the uncertainty can be decreased by about a factor of two with larger statistics, this method includes a model dependence and has an unavoidable basic uncertainty. Several model independent methods have been discussed (using double D_s production, lepton correlations, vertex information, low momentum photons and so on), however these methods mostly require rather large statistics or include a model dependent parameter. Generally, we expect to reduce the f_s uncertainty to $\sim (6 - 8)\%$ with currently available statistics of 23.6 fb^{-1} . The last unknown $f_{B_s^* \bar{B}_s^*}$ value was recently measured with improved accuracy: $f_{B_s^* \bar{B}_s^*} = (90.3^{+3.8}_{-4.0})\%$ [6].

The total uncertainty in the number of B_s^0 is expected to come down from $\sim (15 - 17)\%$ to $\sim (8 - 9)\%$ due to the Belle statistics increase from 1.86 fb^{-1} to 23.6 fb^{-1} . At the moment the most significant uncertainty on the B_s^0 number comes from the f_s uncertainty. It is important to develop a robust method to determine f_s in a model independent way. The uncertainty on the $f_{B_s^* \bar{B}_s^*}$ value is smaller than other uncertainties on the number of B_s^0 and will be further reduced with increasing statistics.

B_s^0 signals can be observed using two variables: the energy difference $\Delta E = E_{B_s^0}^{\text{CM}} - E_{\text{beam}}^{\text{CM}}$ and the beam-energy-constrained mass $M_{\text{bc}} = \sqrt{(E_{\text{beam}}^{\text{CM}})^2 - (p_{B_s^0}^{\text{CM}})^2}$, where $E_{B_s^0}^{\text{CM}}$ and $p_{B_s^0}^{\text{CM}}$ are the energy and momentum of the B_s^0 candidate in the e^+e^- center-of-mass (CM) system, and $E_{\text{beam}}^{\text{CM}}$ is the CM beam energy. The $B_s^* \bar{B}_s^*$, $B_s^* \bar{B}_s^0$, $B_s^0 \bar{B}_s^*$ and $B_s^0 \bar{B}_s^0$ intermediate channels can be distinguished kinematically in the M_{bc} and ΔE plane, where three well-separated B_s^0 signal regions can be defined corresponding to the cases where both, only one, or neither of the B_s^0 mesons originate from a B_s^* decay. The events obtained from MC simulation of the $B_s^0 \rightarrow D_s^- \pi^+$ decay are shown in Fig. 2 for the intermediate $\Upsilon(5S)$ decay channels $B_s^* \bar{B}_s^*$, $B_s^* \bar{B}_s^0$, $B_s^0 \bar{B}_s^*$ and $B_s^0 \bar{B}_s^0$. The signal regions are defined as ellipses corresponding to $\pm(2.0-2.5)\sigma$ (i.e. (95-98)% acceptance) resolution intervals in M_{bc} and ΔE . The signal events from the different intermediate channels are well separated in the M_{bc} and ΔE plane.

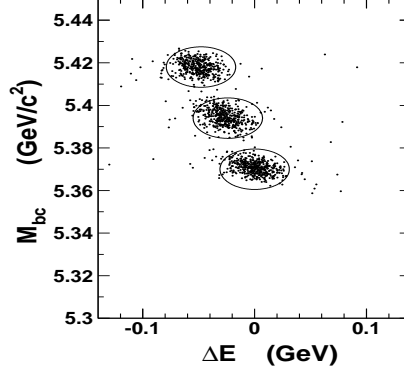


Figure 2: The M_{bc} and ΔE scatter plot for the $B_s^0 \rightarrow D_s^- \pi^+$ decay obtained from the MC simulation. The ellipses show the signal regions for the intermediate $B_s^* \bar{B}_s^*$ (top elliptical region), $B_s^* \bar{B}_s^0$ and $B_s^0 \bar{B}_s^*$ (middle elliptical region), and $B_s^0 \bar{B}_s^0$ (bottom elliptical region) channels.

3. RECENT MEASUREMENTS WITH 23.6 fb^{-1} AT THE $\Upsilon(5S)$

3.1. Measurement of $B_s^0 \rightarrow D_s^- \pi^+$ decay and evidence for $B_s^0 \rightarrow D_s^\mp K^\pm$ decay

We report here the preliminary results from studies of $B_s^0 \rightarrow D_s^- \pi^+$ and $B_s^0 \rightarrow D_s^\mp K^\pm$ decays obtained by the Belle collaboration with 23.6 fb^{-1} at the $\Upsilon(5S)$ [6]. In this analysis D_s^- candidates are reconstructed in the $\phi\pi^-$, $K^{*0}K^-$ and $K_S^0 K^-$ modes. Fig. 3 shows M_{bc} and ΔE scatter plot for the studied decays. A clear signal is observed in the $B_s^0 \rightarrow D_s^- \pi^+$ decay mode, and evidence for the $B_s^0 \rightarrow D_s^\mp K^\pm$ decay is also seen. For each mode, a two-dimensional unbinned extended maximum likelihood fit in M_{bc} and ΔE is performed on the selected candidates. Fig. 4 shows the M_{bc} and ΔE projections in the $B_s^* \bar{B}_s^*$ region of the data, together with the fitted functions.

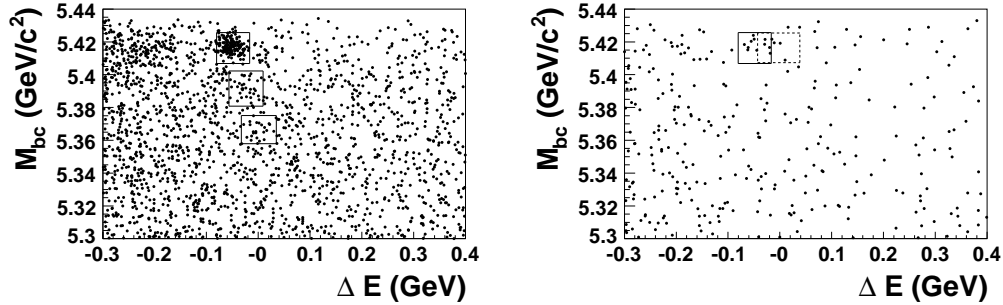


Figure 3: The M_{bc} and ΔE scatter plot for the $B_s^0 \rightarrow D_s^- \pi^+$ (left) and $B_s^0 \rightarrow D_s^\mp K^\pm$ (right) candidates. The three boxes in the left plot are the $\pm 2.5\sigma$ signal regions ($B_s^* \bar{B}_s^*$, $B_s^* \bar{B}_s^0$ and $B_s^0 \bar{B}_s^*$, from top to bottom) while those in the right plot are the $\pm 2.5\sigma$ $B_s^* \bar{B}_s^*$ regions for signal (solid) and for $B_s^0 \rightarrow D_s^- \pi^+$ background (dashed).

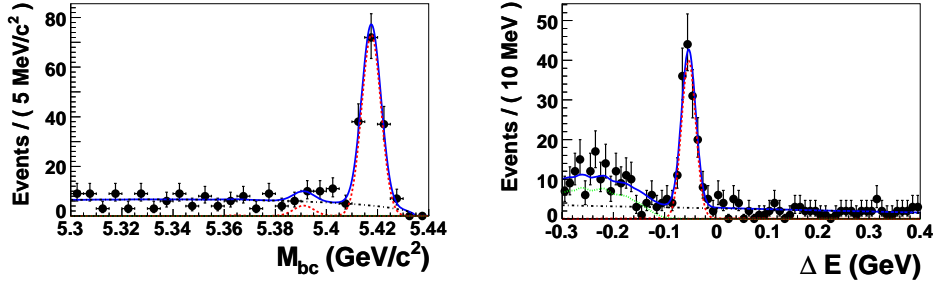


Figure 4: The M_{bc} distribution for $-80 < \Delta E < -17$ MeV region (left) and ΔE distribution for $5.41 < M_{bc} < 5.43$ GeV/ c^2 region (right) for the $B_s^0 \rightarrow D_s^- \pi^+$ candidates. The different fitted components are shown with dashed curves for the signal, dotted curves for the $B_s^0 \rightarrow D_s^{*-} \pi^+$ background, and dash-dotted curves for the continuum.

Finally, the branching fractions $\mathcal{B}(B_s^0 \rightarrow D_s^- \pi^+) = (3.33_{-0.30}^{+0.32}(\text{stat.})_{-0.40}^{+0.41}(\text{syst.}) \pm 0.44(f_s)_{-0.27}^{+0.33}(\mathcal{B}(D_s^- \rightarrow \phi \pi^-))) \times 10^{-3}$ and $\mathcal{B}(B_s^0 \rightarrow D_s^\mp K^\pm) = (2.2_{-0.9}^{+1.1}(\text{stat.}) \pm 0.3(\text{syst.}) \pm 0.3(f_s) \pm 0.2(\mathcal{B}(D_s^- \rightarrow \phi \pi^-))) \times 10^{-4}$ are measured. The ratio $\mathcal{B}(B_s^0 \rightarrow D_s^\mp K^\pm)/\mathcal{B}(B_s^0 \rightarrow D_s^- \pi^+) = (6.5_{-2.9}^{+3.5})\%$ is derived; the errors are completely dominated by the low $B_s^0 \rightarrow D_s^\mp K^\pm$ statistics.

Comparing the number of events reconstructed in the $B_s^0 \rightarrow D_s^- \pi^+$ mode in three signal regions, the fraction of $B_s^* \bar{B}_s^*$ events over all $B_s^{(*)} \bar{B}_s^{(*)}$ events was measured to be $f_{B_s^* \bar{B}_s^*} = (90.3_{-4.0}^{+3.8})\%$. This number is higher than the value of 70% predicted by several theoretical models [7, 8]. From the B_s^0 signal fit the masses $m(B_s^*) = (5317.6 \pm 0.4 \pm 0.5) \text{ MeV}/c^2$ and $m(\bar{B}_s^*) = (5364.6 \pm 1.3 \pm 2.4) \text{ MeV}/c^2$ are obtained. In contrast to theoretical predictions [9] the mass difference $m(B_s^*) - m(\bar{B}_s^*)$ obtained is 2.7σ larger than the world average for $m(B^{*0}) - m(B^0)$.

The distribution of the cosine of the angle between the B_s^0 momentum and the beam axis in the CM system for the $\Upsilon(5S) \rightarrow B_s^* \bar{B}_s^*$ decay (in the $B_s^0 \rightarrow D_s^- \pi^+$ mode) is shown in Fig. 5. The flat shape of this distribution indicates that different spin-momentum combinations contribute in the $\Upsilon(5S) \rightarrow B_s^* \bar{B}_s^*$ decay.

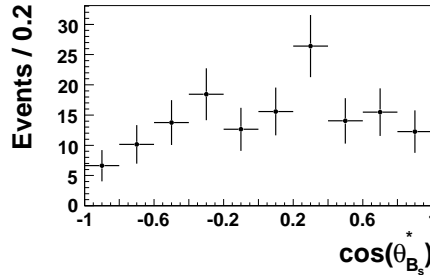


Figure 5: The cosine of the angle between the B_s^0 momentum and the beam axis in the CM system for the $\Upsilon(5S) \rightarrow B_s^* \bar{B}_s^*$ decay.

3.2. Observation of $B_s^0 \rightarrow \phi \gamma$ and search for $B_s^0 \rightarrow \gamma \gamma$ decays

The radiative decays $B_s^0 \rightarrow \phi \gamma$ and $B_s^0 \rightarrow \gamma \gamma$ have been studied at the $\Upsilon(5S)$ with 23.6 fb^{-1} [10]. Only upper limits were obtained for these decays in the previous Belle analysis [4], based on 1.86 fb^{-1} of data.

Within the Standard Model (SM) the $B_s^0 \rightarrow \phi \gamma$ decay can be described by a radiative penguin diagram (Fig. 6, left) and the corresponding branching fraction is predicted to be $\sim 4 \times 10^{-5}$ [11]. The $B_s^0 \rightarrow \gamma \gamma$ decay is expected to proceed via a penguin annihilation diagram (Fig. 6, right) and to have a branching fraction in the range $(0.5 - 1.0) \times 10^{-6}$. However, the $B_s^0 \rightarrow \gamma \gamma$ decay branching fraction is sensitive to some BSM contributions and can be enhanced by about an order of magnitude [12, 13, 14]; such enhanced values are not far from the upper limit expected in this analysis.

The three-dimensional (two-dimensional) unbinned extended maximum likelihood fit to M_{bc} , ΔE and $\cos \theta_\phi^h$ (M_{bc}

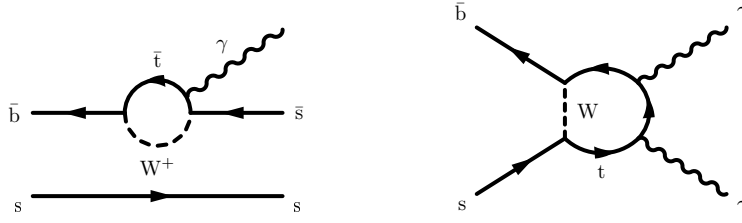


Figure 6: Diagrams describing the dominant SM processes for the $B_s^0 \rightarrow \phi\gamma$ (left) and $B_s^0 \rightarrow \gamma\gamma$ (right) decays.

and ΔE) is performed for $B_s^0 \rightarrow \phi\gamma$ ($B_s^0 \rightarrow \gamma\gamma$) decay to extract the signal yield. Fig. 7 shows the M_{bc} and ΔE projections of the data, together with the fitted functions.

A clear signal is seen in the $B_s^0 \rightarrow \phi\gamma$ mode. This radiative decay is observed for the first time and the branching fraction $\mathcal{B}(B_s^0 \rightarrow \phi\gamma) = (5.7_{-1.5}^{+1.8}(\text{stat.})_{-1.1}^{+1.2}(\text{syst.})) \times 10^{-5}$ is measured. The obtained value is in agreement with the SM predictions. No significant signal is observed in the $B_s^0 \rightarrow \gamma\gamma$ mode, and an upper limit at the 90% C.L. of $\mathcal{B}(B_s^0 \rightarrow \phi\gamma) < 8.7 \times 10^{-6}$ is set.

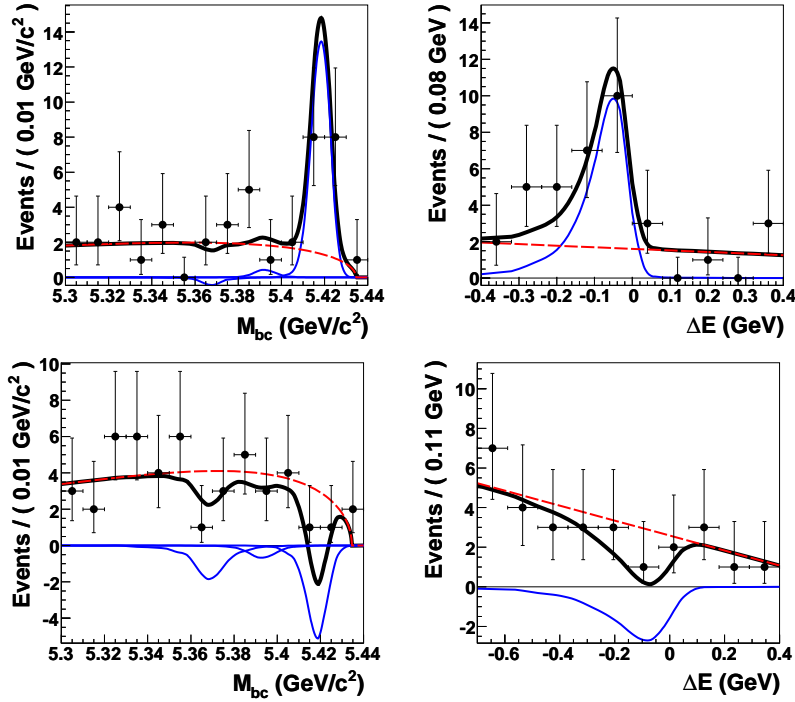


Figure 7: The M_{bc} projection (left) and ΔE projection (right) for the $B_s^0 \rightarrow \phi\gamma$ (top) and $B_s^0 \rightarrow \gamma\gamma$ (bottom) modes. The points with error bars represent data, the thick solid curves are the fit functions, the thin solid curves are the signal functions, and the dashed curves show the continuum contribution. On the M_{bc} figure, signals from $B_s^0\bar{B}_s^0$, $B_s^*\bar{B}_s^0$, and $B_s^*\bar{B}_s^*$ appear from left to right. On the ΔE figure, due to the requirement $M_{bc} > 5.4 \text{ GeV}/c^2$ only the $B_s^*\bar{B}_s^*$ signal contributes.

3.3. First measurement of $B_s^0 \rightarrow X^+\ell^-\nu$ decay

The inclusive semileptonic $B_s^0 \rightarrow X^+\ell^-\nu$ decay branching fraction has been measured for the first time using a 23.6 fb^{-1} data sample collected at the $\Upsilon(5S)$ resonance [15]. This measurement is of special interest, because the total semileptonic B^0 , B^+ and B_s^0 branching fractions, together with corresponding well-measured lifetimes, determine the semileptonic widths. These widths for the B^0 , B^+ and B_s^0 mesons are expected to be equal, neglecting small corrections due to electromagnetic and light quark mass difference effects. If any significant difference between the B^0 ,

B^+ and B_s^0 semileptonic widths were observed, it would indicate a previously unknown source of lepton production in B decays. On the other hand, assuming equal semileptonic widths in $B^{0/+}$ and B_s^0 decays, the inclusive B_s^0 semileptonic branching fraction can be directly related to the B_s^0 lifetime. This can be potentially useful taking into account a possible CP correlation of the B_s^0 mesons produced in $\Upsilon(5S)$ decays.

The correlated production of a D_s^+ meson and a same-sign lepton at the $\Upsilon(5S)$ resonance is used in this analysis to measure $\mathcal{B}(B_s^0 \rightarrow X^+ \ell^- \nu)$. D_s^+ candidates are reconstructed in a clean $\phi\pi^+$ mode. First, we selected the data sample with D_s^+ mesons and then studied the same-sign lepton production in this sample. Neither the $c\bar{c}$ continuum nor $B^{(*)}\bar{B}^{(*)}$ states (except for a small contribution due to $\sim 19\%$ B^0 mixing effect) can result in a same-sign c -quark (i.e., D_s^+ meson) and primary lepton final state.

The final leptonic momentum distributions produced in B_s^0 decays (Fig. 8) obtained after background subtractions and an efficiency correction are used to extract the numbers of primary and secondary leptons. The backgrounds are subtracted using continuum and $\Upsilon(4S)$ data to estimate continuum and $B\bar{B}$ contributions. The MC simulation is used to obtain the momentum distribution shapes for leptons from primary B_s decays and from secondary D_s^+ , D^0 , D^+ or τ^+ decays. We fit the data with a function which includes the sum of these two terms with fixed shapes and floating normalizations.

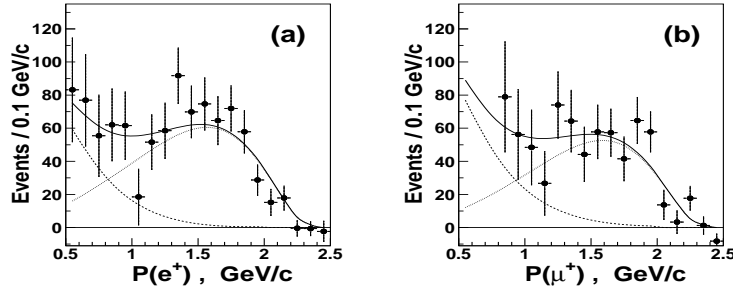


Figure 8: The electron (a) and muon (b) momentum distributions from B_s^0 decays. The solid curves show the results of the fits, and the dotted curves show the fitted contributions from primary and secondary leptons.

Finally, we obtained the semileptonic branching fractions:

$$\begin{aligned}
 \mathcal{B}(B_s^0 \rightarrow X^+ e^- \nu) &= (10.9 \pm 1.0 \pm 0.9)\% \\
 \mathcal{B}(B_s^0 \rightarrow X^+ \mu^- \nu) &= (9.2 \pm 1.0 \pm 0.8)\% \\
 \mathcal{B}(B_s^0 \rightarrow X^+ \ell^- \nu) &= (10.2 \pm 0.8 \pm 0.9)\%,
 \end{aligned}
 \tag{1}$$

where the latter one represents an average over electrons and muons. The obtained branching fractions can be compared with the PDG value $\mathcal{B}(B^0 \rightarrow X^+ \ell^- \nu) = (10.33 \pm 0.28)\%$ [5], which is theoretically expected to be approximately the same, neglecting a small possible lifetime difference and small corrections due to electromagnetic and light quark mass difference effects.

3.4. Observation of $\Upsilon(5S) \rightarrow \Upsilon(1S) \pi^+ \pi^-$ and $\Upsilon(5S) \rightarrow \Upsilon(2S) \pi^+ \pi^-$ decays

The production of $\Upsilon(1S) \pi^+ \pi^-$, $\Upsilon(2S) \pi^+ \pi^-$, $\Upsilon(3S) \pi^+ \pi^-$, and $\Upsilon(1S) K^+ K^-$ final states in a 21.7 fb^{-1} data sample obtained at $e^+ e^-$ collisions with CM energy near the peak of the $\Upsilon(5S)$ resonance has been studied by Belle [16]. Final states with two opposite-sign muons and two opposite-sign pions (or kaons) are selected. The signal candidates are identified using the kinematic variable ΔM , defined as the difference between $M(\mu^+ \mu^- \pi^+ \pi^-)$ or $M(\mu^+ \mu^- K^+ K^-)$ and $M(\mu^+ \mu^-)$ for pion or kaon modes. In the studied processes the opposite-sign muon pair should have a mass in the nominal $\Upsilon(1S)$, $\Upsilon(2S)$ or $\Upsilon(3S)$ mass regions.

Figure 9 (left) shows the two-dimensional scatter plots of $M(\mu^+ \mu^-)$ vs ΔM . Horizontal shaded bands correspond to $\Upsilon(1S)$, $\Upsilon(2S)$ or $\Upsilon(3S)$ (only $\Upsilon(1S)$ for (b)), and open boxes are the fitting regions for $\Upsilon(5S) \rightarrow \Upsilon(nS) \pi^+ \pi^-$ and

$\Upsilon(5S) \rightarrow \Upsilon(1S) K^+ K^-$. The region where the mass of $\mu^+ \mu^- \pi^+ \pi^-$ (or $\mu^+ \mu^- K^+ K^-$) combination corresponds to the $\Upsilon(5S)$ CM energy of 10869 MeV is tilted in the $M(\mu^+ \mu^-)$ vs ΔM plot. Fig. 9 (right) shows the ΔM projections for $\mu^+ \mu^- \pi^+ \pi^-$ events in the $\Upsilon(1S)$ (a) and $\Upsilon(2S)$ (b) regions.

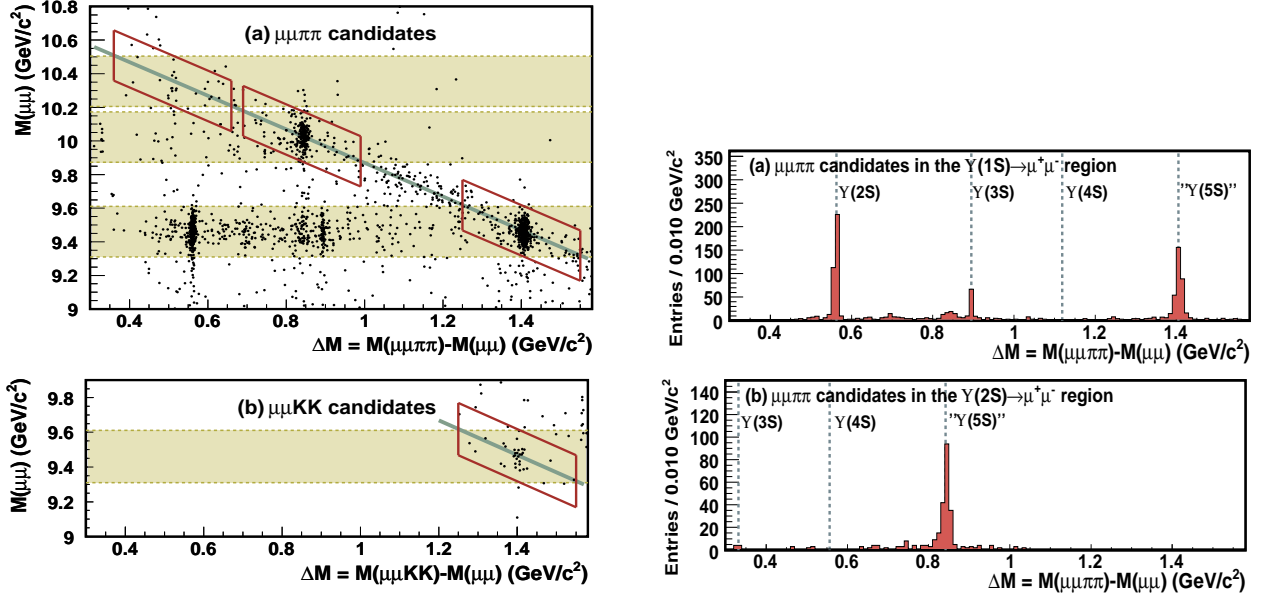


Figure 9: Scatter plot of $M(\mu^+ \mu^-)$ vs ΔM for the data collected at $\sqrt{s} \sim 10.87$ GeV, for (a, left) $\mu^+ \mu^- \pi^+ \pi^-$ and (b, left) $\mu^+ \mu^- K^+ K^-$ candidates. Horizontal shaded bands correspond to $\Upsilon(1S)$, $\Upsilon(2S)$ or $\Upsilon(3S)$ (only $\Upsilon(1S)$ for (b)), and open boxes are the fitting regions for $\Upsilon(5S) \rightarrow \Upsilon(nS) \pi^+ \pi^-$ and $\Upsilon(5S) \rightarrow \Upsilon(1S) K^+ K^-$. The ΔM projections in the $\Upsilon(1S)$ (a, right) and $\Upsilon(2S)$ (b, right) regions are also shown. Vertical dashed lines show the expected ΔM values for the $\Upsilon(nS) \rightarrow \Upsilon(1, 2S) \pi^+ \pi^-$ transitions.

The obtained branching fractions and partial widths are given in Table 1. For comparison, the partial widths for similar transitions from $\Upsilon(2S)$, $\Upsilon(3S)$, or $\Upsilon(4S)$ are also shown. The $\Upsilon(5S)$ partial widths (assuming that the signal events are solely due to the $\Upsilon(5S)$ resonance) are found to be in the range (0.52-0.85) MeV, that is more than 2 orders of magnitude larger than the corresponding partial widths for $\Upsilon(2S)$, $\Upsilon(3S)$, or $\Upsilon(4S)$ decays. The unexpectedly large $\Upsilon(5S)$ partial widths disagree with the expectation for a pure $b\bar{b}$ state, unless there is a new mechanism to enhance the decay rates.

Table I: The branching fractions (\mathcal{B}) and the partial widths (Γ) for $\Upsilon(nS) \rightarrow \Upsilon(mS) \pi^+ \pi^-$ and $\Upsilon(1S) K^+ K^-$ processes are listed. The first error is statistical, and the second is systematic. The values for the $\Upsilon(2,3,4S)$ decays are from [5].

Process	\mathcal{B} (%)	Γ (MeV)	Process	Γ (MeV)
$\Upsilon(5S) \rightarrow \Upsilon(1S) \pi^+ \pi^-$	$0.53 \pm 0.03 \pm 0.05$	$0.59 \pm 0.04 \pm 0.09$	$\Upsilon(2S) \rightarrow \Upsilon(1S) \pi^+ \pi^-$	0.006
$\Upsilon(5S) \rightarrow \Upsilon(2S) \pi^+ \pi^-$	$0.78 \pm 0.06 \pm 0.11$	$0.85 \pm 0.07 \pm 0.16$	$\Upsilon(3S) \rightarrow \Upsilon(1S) \pi^+ \pi^-$	0.0009
$\Upsilon(5S) \rightarrow \Upsilon(3S) \pi^+ \pi^-$	$0.48^{+0.18}_{-0.15} \pm 0.07$	$0.52^{+0.20}_{-0.17} \pm 0.10$	$\Upsilon(4S) \rightarrow \Upsilon(1S) \pi^+ \pi^-$	0.0019
$\Upsilon(5S) \rightarrow \Upsilon(1S) K^+ K^-$	$0.061^{+0.016}_{-0.014} \pm 0.010$	$0.67^{+0.017}_{-0.015} \pm 0.013$		

4. PHYSICS PROSPECTS AT THE $\Upsilon(5S)$

4.1. Physics with (20-200) fb^{-1} at the $\Upsilon(5S)$

Data at the $\Upsilon(5S)$ have many advantages for B_s^0 studies compared to hadron-hadron collisions (in particular with the CDF and D0 experiments at Tevatron), such as high photon and π^0 reconstruction efficiency, trigger efficiency of almost 100% for hadronic modes and excellent charged kaon and pion identification. A model-independent determination of the number of initial B_s^0 mesons at $\Upsilon(5S)$ data samples opens an opportunity for precise absolute B_s^0 branching fraction measurements. The possibility of partial reconstruction of specific B_s^0 decays and measurements of inclusive B_s^0 processes are additional advantages of e^+e^- colliders running at the $\Upsilon(5S)$. On the other hand, lower B^0 and B^+ meson production rates at the $\Upsilon(5S)$ compared to that at the $\Upsilon(4S)$, the smaller number of produced B_s^0 mesons compared to the Tevatron experiments, and insufficient accuracy of the B_s^0 vertex reconstruction to observe $B_s^0 - \bar{B}_s^0$ mixing are the main disadvantages of running at the $\Upsilon(5S)$.

Developing our current and future physics programs at the $\Upsilon(5S)$ is based on the advantages. The currently available statistics of 23.6fb^{-1} at the $\Upsilon(5S)$ allows to perform many interesting B_s^0 studies. The list of decays where significant signals are expected to be observed include the following modes:

- $B_s^0 \rightarrow D_s^- \rho^+$ and $B_s^0 \rightarrow D_s^- a_1^+$.
- $B_s^0 \rightarrow J/\psi \phi$, $B_s^0 \rightarrow J/\psi \eta$ and $B_s^0 \rightarrow J/\psi \eta'$.
- $B_s^0 \rightarrow D_s^{(*)-} D_s^{(*)+}$.
- $B_s^0 \rightarrow D_{sJ}^- \pi^+$.
- $B_s^0 \rightarrow K^- K^+$.
- $B_s^0 \rightarrow D^0 K_S^0$, $B_s^0 \rightarrow D^0 K^{*0}$.
- $B_s^0 \rightarrow D_s^- \ell^+ \nu$, $B_s^0 \rightarrow D_s^{*-} \ell^+ \nu$.

Combining modes with the large number of reconstructed B_s^0 mesons, the B_s^0 lifetime can be measured with high precision. The production ratios for different $B^{(*)} \bar{B}^{(*)} n\pi$ and $B_s^{(*)0} \bar{B}_s^{(*)0}$ channels can be also determined. It could be potentially interesting to take a small data sample at a higher e^+e^- CM energy, there the B^{**} or even B_s^{**} signals could emerge. A dedicated energy scan at a $\Upsilon(5S)$ and $\Upsilon(6S)$ energy region is an excellent tool to search for new $b\bar{b}$ states. If our $\Upsilon(5S)$ data sample will be increased to $(100-200) \text{fb}^{-1}$, several rare B_s^0 decays can be potentially measured; the most promising modes are $B_s^0 \rightarrow K^- \rho^+$, $B_s^0 \rightarrow \eta\eta$, $B_s^0 \rightarrow \eta\eta'$ and $B_s^0 \rightarrow \phi\phi$.

4.2. Feasibility of $\Delta\Gamma_s/\Gamma_s$ measurement

A new generation of B -factories with luminosity 20-100 times higher than that delivered to the Belle and BaBar experiments has been recently proposed [17, 18]. Taking into account an average integrated luminosity of about 1fb^{-1} per day taken by Belle in first $\Upsilon(5S)$ runs, an integrated luminosity of 1000fb^{-1} can be taken by future B -factories in 10-50 days. Although many interesting rare B_s^0 decays, such as $B_s^0 \rightarrow \gamma\gamma$ and $B_s^0 \rightarrow D_s^- K^+$, can be measured with such a data sample, we would like to focus here on a few of the most important tasks. First of all, simple estimates indicate that the $\Delta\Gamma_s/\Gamma_s$ measurement can be performed with a 1ab^{-1} data sample.

Although the $\Delta\Gamma_s/\Gamma_s$ measurement itself is important, a comparison of the direct B_s^0 width difference measurement with that calculated using the $\mathcal{B}(B_s^0 \rightarrow D_s^{(*)-} D_s^{(*)+})$ measurement is the most important goal for such a study because it provides a critical Standard Model test. This method was developed by Grossman [19]; a more detailed description can be found in [20]. Technically we expect to have $\sim(5-7)\%$ accuracy in the $\mathcal{B}(B_s^0 \rightarrow D_s^{(*)-} D_s^{(*)+})$ measurement with 1ab^{-1} . Therefore the accuracy of the SM test depends mostly on the uncertainty in the direct $\Delta\Gamma_s/\Gamma_s$ measurement.

We propose a simple method to determine the $\Delta\Gamma_s/\Gamma_s$ value based on a measurement of the distance between two B_s^0 vertices. We assume fully anti-correlated CP values of the two final state B_s^0 mesons in the decay channel

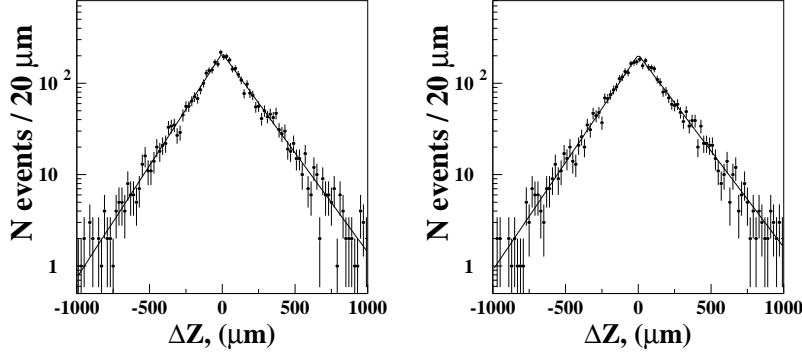


Figure 10: The MC simulated ΔZ distributions between two B_s^0 vertices are shown for the single vertex resolution neglected (left) or modeled by a Gaussian with $\sigma = 40\mu\text{m}$ (right). Full curves show the results of fits described in the text.

$\Upsilon(5S) \rightarrow B_s^* \bar{B}_s^*$. To estimate the uncertainty of $\Delta\Gamma_s/\Gamma_s$ measurement with 1 ab^{-1} of data at the $\Upsilon(5S)$, we use a toy MC simulation to model the distance between two B_s^0 decay vertices (Fig. 10). The number of fully reconstructed B_s^0 mesons with a data sample of 1 ab^{-1} is estimated to be effectively ~ 4000 events. This sample is expected to comprise $\sim 1000 D_s^{(*)-} D_s^{(*)+}$ events, $\sim 1500 J/\psi \eta/\eta'$ events, $\sim 600 K^+ K^-$ events and $\sim 2200 J/\psi\phi$ events. The $J/\psi\phi$ events contain $\sim 20\%$ CP -odd and $\sim 80\%$ CP -even components, and we reduce this effective event number to ~ 1000 .

Assuming CP conservation in B_s^0 decays, the mass eigenstates are CP -eigenstates, and one could compare the lifetime distributions of a B_s^0/\bar{B}_s^0 decaying to CP -even and CP -odd final state. To measure the $\Delta\Gamma_s = \Gamma_L - \Gamma_S$ value experimentally (Γ_L and Γ_S are widths of long-lived and short-lived B_s^0 mesons), we should select all reconstructed B_s^0 decays with fixed CP , and determine the decay vertices for this B_s^0 with fixed CP and for the second B_s^0 in the event. Then we can measure the distance between the decay vertices $\Delta Z = Z_{CP\text{even}} - Z_{CP\text{odd}}$ along the $\Upsilon(5S)$ boost direction and, respectively, the time difference $\Delta t = \Delta Z/(\beta\gamma c)$ (here $\beta\gamma$ is the boost factor). The expected distribution is proportional to $\exp(-\Gamma_L \Delta t)$ for $\Delta t > 0$ and $\exp(+\Gamma_S \Delta t)$ for $\Delta t < 0$; thus, fitting to this distribution yields both Γ_L and Γ_S .

Finally, from the ΔZ distribution fit we obtained the value $\Delta\Gamma_s/\Gamma_s = (10.2 \pm 2.4)\%$ (significance $\sim 4\sigma$), where value $\Delta\Gamma_s/\Gamma_s = 10.0\%$ was fixed in the toy MC simulation. Because background contribution is low in the studied modes, the signal significance depends on statistics as $\propto \sqrt{L_{\text{int}}}$. The vertex resolution effect is negligible: almost no degradation in accuracy of $\Delta\Gamma_s$ measurement was found comparing the ΔZ distribution fit values with the vertex resolution neglected (Fig. 10, left) in toy MC simulation and the single vertex resolution of $\sim 40\mu\text{m}$ (Fig. 10, right) included in toy MC, latter reproduces roughly the current Belle vertex reconstruction uncertainty in ΔZ . It is interesting that we can use the event numbers N^+ and N^- in the $\Delta Z > 0$ and $\Delta Z < 0$ regions, respectively, to estimate $\Delta\Gamma_s/\Gamma_s = 2 \times (N^+ - N^-) / (N^+ + N^-)$, however the statistical uncertainty is $\sim 30\%$ larger in this method.

4.3. Feasibility of $B_s^0 - \bar{B}_s^0$ mixing measurement with improved vertex resolution

Theoretically almost zero CP violation is expected in B_s^0 mixing within the Standard Model, therefore, the search for the CP violation provides an important opportunity to observe effects Beyond the Standard Model. It is interesting to note that the conventional method of time dependent CP violation measurement is often assumed to be impossible at the $\Upsilon(5S)$ due to very fast B_s^0 oscillations. However this may be possible, since the corresponding distance between oscillation function maximum and minimum at the $\Upsilon(5S)$ is $D = \pi \cdot \Delta m_s \cdot \beta\gamma c = 22.5\mu\text{m}$. Such decay vertex resolution can be reached by existing vertex detectors: currently discussed Super Belle single vertex resolution (SVR) is expected to be $\sim 20\mu\text{m}$ for tracks with momentum greater than $1.5\text{ GeV}/c$ and direction nearly perpendicular to the beam axes.

The B_s^0 oscillations can be observed using the same-sign (SS) and opposite-sign (OS) high momentum leptons (their intersections with beam profile can be used to obtain vertex positions) produced in two semileptonic B_s^0 decays

from the $\Upsilon(5S) \rightarrow B_s^{(*)0} \bar{B}_s^{(*)0}$ decay. The number of SS and OS events is very large in 1 ab^{-1} data sample and is not critical for such an analysis. In Fig. 11 the MC simulated ΔZ distributions with 1 ab^{-1} dataset are shown for (from left to right) SS lepton events with $\text{SVR} = 10 \mu\text{m}$, SS-OS event difference with $\text{SVR} = 10 \mu\text{m}$, SS lepton events with $\text{SVR} = 13 \mu\text{m}$, and SS-OS event difference with $\text{SVR} = 13 \mu\text{m}$. Oscillations are perfectly seen with $\text{SVR} = 10 \mu\text{m}$, but the sinusoidal shape begins to disappear at $\text{SVR} = 13 \mu\text{m}$. Therefore, to measure B_s^0 mixing at Super Belle the SVR should be improved to $\sim 15 \mu\text{m}$ or a $\Upsilon(5S)$ boost value should be increased by at least 25%.

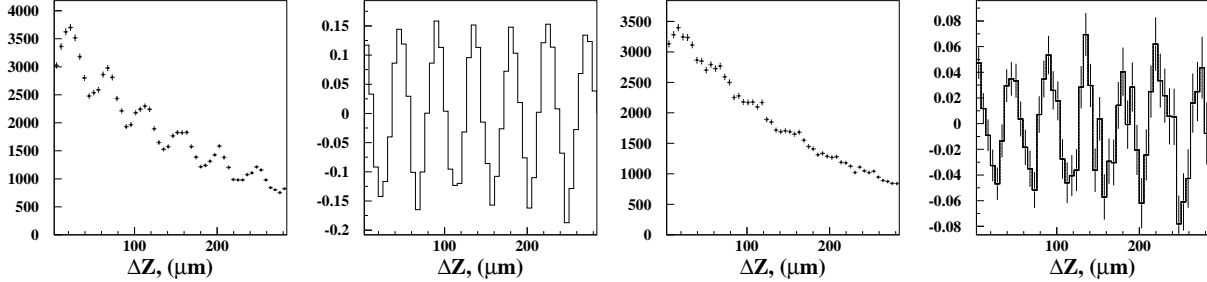


Figure 11: The event numbers for SS leptons (first) and event number difference for SS and OS leptons (second) as a function of ΔZ is shown for $\text{SVR} = 10 \mu\text{m}$ (two left), and for $\text{SVR} = 13 \mu\text{m}$ (two right). The distributions are simulated using toy MC.

4.4. Potential measurements with higher beam energies

One of the significant advantages of hadron-hadron colliders is the possibility to study many heavy beauty states, such as B^{**} , B_s^{**} , B_c , Λ_b , Σ_b et. al. Potentially, however, all these states can be studied at the e^+e^- collider running at the center-of-mass energy (12-14) GeV. Even outside Υ resonances, the $b\bar{b}$ continuum is expected to be $\sim 10\%$ of all continuum events. In particular, the Λ_b baryons could be produced at the center-of-mass energy of $\sim 11.3 \text{ GeV}$ (threshold for $\Lambda_b \bar{\Lambda}_b$ pair production is $E = 11.248 \text{ GeV}$) with approximately the same rate as B_s^0 mesons. In a very high luminosity B -factory with a wide allowed beam energy range, the study of B_c mesons seems to be also possible.

In conclusion, we discussed recent results and future prospects for the $\Upsilon(5S)$ running at B -factories. Many new results are obtained with the 23.6 fb^{-1} data sample collected by Belle at the $\Upsilon(5S)$ and more results are expected soon. The results obviously demonstrate that B_s^0 meson studies at the $\Upsilon(5S)$ have a great potential. It is important to have a large allowed range of beam energies and a high performance vertex detector at future Super B -factories. Important tests of the Standard Model can be performed with statistics of the order of 1 ab^{-1} at the $\Upsilon(5S)$.

References

- [1] M. Artuso *et al.* (CLEO Collaboration), Phys. Rev. Lett. **95**, 261801, 2005.
- [2] G. Bonvicini *et al.* (CLEO Collaboration), Phys. Rev. Lett. **96**, 022002, 2006.
- [3] A. Drutskoy *et al.* (Belle Collaboration), Phys. Rev. Lett. **98**, 052001, 2007.
- [4] A. Drutskoy *et al.* (Belle Collaboration), Phys. Rev. D **76**, 012002, 2007.
- [5] W.-M. Yao *et al.* (Particle Data Group), J. Phys. G **33**, 1, 2006.
- [6] R. Louvot *et al.* (Belle Collaboration), the preliminary results will be presented on ICHEP08.
- [7] A. G. Grozin, and M. Neubert, Phys. Rev. D **55**, 272, 1997.
- [8] N. A. Törnqvist, Phys. Rev. Lett. **53**, 878, 1984.
- [9] W. Bardeen, E. Eichten, and C. Hill, Phys. Rev. D **68**, 054024, 2003.
- [10] J. Wicht *et al.* (Belle Collaboration), Phys. Rev. Lett. **100**, 121801, 2008.
- [11] P. Ball, G. W. Jones, and R. Zwicky, Phys. Rev. D **75**, 054004, 2007.
- [12] A. Gemintern, S. Bar-Shalom, and G. Eilam, Phys. Rev. D **70**, 035008, 2004.

- [13] W. J. Huo, C. D. Lu, and Z. J. Xiao, arXiv:hep-ph/0302177, 2003.
- [14] T. M. Aliev, and E. O. Iltan, Phys. Rev. D **58**, 095014, 1998.
- [15] K. Abe *et al.* (Belle Collaboration), arXiv:hep-ph/0710.2548, 2007.
- [16] K.-F. Chen *et al.* (Belle Collaboration), Phys. Rev. Lett. **100**, 112001, 2008.
- [17] A. G. Akeroyd *et al.* (SuperKEKB Physics Working Group), arXiv:hep-ex/0406071, 2004.
- [18] M. Bona *et al.* (SuperB Collaboration), arXiv:hep-ex/0709.0451, 2007.
- [19] Y. Grossman, Phys. Lett. B **380**, 99, 1996.
- [20] I. Dunietz, R. Fleischer, and U. Nierste, Phys. Rev. D **63**, 114015, 2001.